

Open camera or QR reader and scan code to access this article and other resources online.



# Retinoic Acid Influences *connexin43* Expression During Joint Formation in the Regenerating Zebrafish Fin

Alexander W. Seaver, BA, Noah S. Weaver, BS, and M. Kathryn Iovine, PhD

## Abstract

**Background:** The regenerating zebrafish fin skeleton is comprised of multiple bony fin rays, each made of alternating bony segments and fin ray joints. This pattern is regulated by the gap junction protein Connexin43 (Cx43), which provides instructional cues to skeletal precursor cells (SPCs). Elevated Cx43 favors osteoblast differentiation and disfavors joint forming cell differentiation. The goal of this article is to test if retinoic acid (RA) contributes to the regulation of *cx43* expression.

**Materials and Methods:** Functional studies inhibiting the RA-synthesizing enzyme *Adh1a2* were evaluated using *in situ* hybridization to monitor gene expression and with measurements of the length of fin ray segments to monitor impacts on SPC differentiation and joint formation.

**Results:** *Adh1a2*-knockdown leads to reduced expression of *cx43* and increased expression of *evx1*, a gene required for joint formation. Additionally, inhibition of *Adh1a2* function leads to short fin ray segments. We also find evidence for synergy between *aldh1a2* and *cx43*, suggesting that these genes function in a common molecular pathway to regulate joint formation.

**Conclusions:** The role of RA is to promote *cx43* expression in the regenerating fin to regulate joint formation and the length of bony fin ray segments. We suggest that RA signaling must coordinate with additional pathways that also regulate *cx43* transcription.

**Keywords:** Connexin43, retinoic acid, skeletal regeneration, joint formation, zebrafish

## Introduction

PATTERNING OF THE skeleton requires appropriately sized bones and correct positioning of joints. The determination of joint location is poorly understood. The zebrafish regenerating fin has been used as a model to address this question. The zebrafish fin is comprised of multiple bony fin rays, and each fin ray is segmented. Thus, each bony segment is flanked by joints. Regeneration proceeds rapidly following amputation and is complete in about 2–3 weeks.<sup>1</sup> Wound healing occurs in the first 24 h postamputation (hpa), followed by blastema formation, and next by outgrowth and differentiation. Within each fin ray, the dividing cells of the blastema are located in the medial mesenchyme, while skeletal differentiation occurs in the lateral mesenchyme.

Osteoblasts and joint-forming cells (JFCs) are derived from a common skeletal precursor cell (SPC).<sup>2</sup> SPCs that will

become JFCs upregulate the even-skipped transcription factor *evx1*, which is required for joint formation.<sup>3,4</sup> Because joint formation occurs when SPCs differentiate into JFCs, and because the length of bony fin ray segments depends on the timing of joint formation, we use segment length as a proxy for joint formation.

Prior research has shown that gap junction intercellular communication (GJIC) via Connexin43 (Cx43) gap junctions influences joint formation. For example, the *short fin* (*sof*<sup>*b123*</sup>) mutant has short fin ray segments (i.e., due to premature joint formation) caused by hypomorphic mutations in *cx43*.<sup>5</sup> Interestingly, inhibiting Cx43-GJIC via the GAP27 peptide inhibitor<sup>6</sup> recapitulates the *sof*<sup>*b123*</sup> phenotype.<sup>7</sup> Moreover, the *cx43*<sup>*th10*</sup> mutant expresses a gain-of-function allele of *cx43* and has long fin ray segments (i.e., due to delayed joint formation). This long segment phenotype is rescued by GAP27.<sup>7</sup> These and other findings indicate that Cx43-GJIC inhibits

joint formation. Clonal analyses were performed to identify the cells in which Cx43-GJIC is required. It was determined that Cx43 function in the medial mesenchyme controls segment length.<sup>8</sup> Thus, Cx43-GJIC acts nonautonomously to inhibit joint formation, and thereby regulate segment length.

Because Cx43-GJIC inhibits joint formation, it must be periodically abrogated to permit JFC differentiation. Indeed, *cx43* mRNA levels are reduced coincident with the initiation of joint formation.<sup>8</sup> The expression of *cx43* was monitored at pre-joint initiation (72 hpa), at joint initiation (87 hpa), and at post-joint initiation (96 hpa); *cx43* mRNA is reduced at 87 hpa. Importantly, expression of *evx1* exhibited the inverse pattern and was elevated at 87 hpa. Moreover, manipulating *cx43* mRNA levels in the joint formation timeline was sufficient to influence *evx1* and joint formation. Together, these results indicate that Cx43-GJIC suppresses joint formation by suppressing *evx1*, and that the amount of Cx43-GJIC (i.e., regulated in part by the amount of *cx43* mRNA) is reduced at the time of joint initiation. Taken further, oscillations of *cx43* mRNA may determine the alternating pattern of bony segments (elevated *cx43*) and fin ray joints (reduced *cx43*). It is therefore of interest to define the mechanisms that determine the relative level of *cx43* transcription in the regenerating fin.

Because treatment of regenerating fins with retinoic acid (RA) also appears to inhibit *evx1*,<sup>9</sup> RA is a likely candidate for regulating *cx43* expression. This possibility has not been tested. The goal of this work is to determine if RA contributes to the regulation of *cx43* expression during joint formation.

## Materials and Methods

### Fish maintenance

*Danio rerio* were maintained in a circulating water system (Aquatic Habitats) in accordance with previously described conditions.<sup>7</sup> Animal handling was performed in accordance with the Institutional Animal Care and Use Committee guidelines for Lehigh University (Protocol #256).

### Zebrafish strains

We used an equal number of wild-type (WT) and *sof*<sup>b123</sup> male and female fish aged between 6 and 18 months age matched within each experiment. Caudal fin amputations were performed using 0.1% tricaine anesthesia solution. For monitoring gene expression during the joint formation timeline, amputations were performed at the 33% level as described.<sup>8</sup> All other amputations were performed at the 50% level. Fish recovered in fresh water following amputation.

### In situ hybridization

*In situ* hybridization (ISH) was performed on fins fixed in 4% paraformaldehyde/phosphate-buffered saline for 4 h at room temperature and dehydrated in 100% methanol at -20°C for at least 24 h. Antisense digoxigenin-labeled probes were generated as described (*evx1*<sup>3</sup>; *cx43*<sup>5</sup>; *shh*<sup>10</sup>). Whole-mount ISH was performed as described.<sup>11</sup> Three independent trials of at least five fins per trial were completed.

### Protein lysates and immunoblotting

Fins were amputated, as described above, and harvested 24 h posttreatment (hpt). Regenerates of three fins were pooled

into 1.5 mL Eppendorf tubes and placed on ice. Fins were then fixed with a 1:1 solution of heptane and methanol for 5 min on a rocker. Fins were then washed twice with methanol and subsequently twice with embryo buffer.<sup>12</sup> After removing the supernatant, 50  $\mu$ L embryo buffer and 1  $\mu$ L Protein Inhibitor Cocktail was added and fins were manually homogenized with pestles (Fisher 12-141-363) on ice. Next, 50  $\mu$ L 5 $\times$ sodium dodecyl-sulfate loading buffer was added, and samples were heated to 95°C for 5 min and loaded on 10% sodium dodecyl-sulfate polyacrylamide gel electrophoresis gels.

Following electrophoresis, gels were washed briefly in Tris-buffered saline with Tween-20 (TBST) and transferred using a Trans-Blot Turbo Transfer System (BIO RAD). After transfer, blots were washed briefly with TBST then incubated in 5% bovine serum albumin (BSA)/TBST for 1 h. Blots were then incubated overnight at 4°C in anti-Aldh1a2 antibody (1:500; GeneTex GTX124302) and anti- $\alpha$ -Tubulin (1:1000; Sigma T6074) in 5% BSA/TBST. Secondary fluorophore-tagged antibodies were incubated with the blots the following day (1:1000 donkey anti-rabbit Alexa Fluor 647; Invitrogen A-31573 and 1:1000 goat anti-mouse Alexa Fluor 488; Invitrogen A-11001) in TBST. Imaging was performed on the ChemiDoc MP Imaging System (BIO RAD). Band intensity analysis was performed using ImageJ (NIH).

### Morpholino-mediated gene knockdown

Morpholinos (MOs) were tagged with fluorescein to permit confirmation of cellular uptake and purchased from Gene Tools, LLC (ATG-MO-CTGGAGGTCATCGCGTCTATTGAA; SB-MO-ACAGGGCCAAAACACTCACAGGAAT). Standard control MO (SC-MO) was used as a negative control. Micro-injection and electroporation procedures were performed as described previously.<sup>13</sup> Twenty-four hours postinjection and electroporation, the fins were evaluated for MO uptake by checking for fluorescence using an X-Cite 120 Illumination System (EXFO) connected to a Nikon Eclipse 80i imaging microscope. Fluorescein-positive fins were evaluated for gene expression changes at 4 dpa/1 dpi via ISH, for protein levels by Western blot at 5 dpa/1 dpi, and for segment length at 7 dpa/4 dpi.

### cDNA synthesis and quantitative RT-PCR

Total RNA was isolated from 5 dpa caudal fin regenerates (6 per replicate, 3 replicates) using Trizol. cDNA was synthesized from 1  $\mu$ g of total RNA with SuperScript III reverse transcriptase (Invitrogen 56575) and oligo dT primers (Invitrogen 5730G). cDNA was diluted 1:10 in sterile dH<sub>2</sub>O before use in quantitative RT-PCR (qPCR). Primers used were as follows: *cx43* (F: 5'-TCGCGTACTTGGATTTG GTGA-3'; R: 5'-CCTTGTC AAGAAGCCTTCCCA-3'), *evx1* (F: 5'-TTGGCGGCTGCCTTAAATT-3'; R: 5'-TGTCC TTCATGCGACGGTT-3'), *aldh1a2* (F: 5'-GCTGATGTG GATAAAGCTGT-3'; R: 5'-ACTCCAGGGTAGCAAGG TAA-3'), and as a housekeeping gene, *keratin4* (F: 5'-TCATCGACAAAGTGCCTTC-3'; R: 5'-TCGATGTTG GAACGTGTGGT-3').

The 2 $\times$ QuantiNova SYBR Green PCR Master Mix (Qiagen 1076717) was used. Analysis was done using Rotor-Gene 6000 thermocycler and software (Corbette Research). The average cycle number (C<sub>T</sub>) for each gene was normalized to *keratin4* C<sub>T</sub> values to give  $\Delta$ C<sub>T</sub> values. For each gene of interest, the  $\Delta$ C<sub>T</sub> value of the control group was then

subtracted from the  $\Delta C_T$  value of the experimental group to give the  $\Delta\Delta C_T$  value which represents the normalized difference in  $C_T$  between the groups. Finally, fold difference is reported as the value  $2^{(-\Delta\Delta C_T)}$ .

### Segment length

Bony segments and fin ray joints were visualized using the vital dye calcein.<sup>14</sup> Fish were allowed to swim for 1 h in 0.02% calcein (pH 7.4) in a dark closet at room temperature, then returned to fresh water which was changed every 5 min for a total of 15 min. Fish were anesthetized using tricaine and imaged using a Nikon Eclipse 80i imaging microscope and NIS Elements BR 4.60.00 software. Measurement was taken on the third-most dorsal or ventral ray of the caudal fin as previously established.<sup>15</sup> Segments were measured as the distance from the first joint formed in the regenerate to the second joint.

### Pharmacological inhibition of Aldh1a2 activity

The ALDH1 inhibitor WIN-18446 (Tocris 4736) was dissolved to a stock solution of 12.5 mM in dimethyl sulfoxide (DMSO) and diluted to the appropriate concentration (i.e., 100 or 500 nM) in 500 mL of fish system water. Fish with 3 dpa regenerating fins were placed in either WIN-18446-treated water or water containing an equal concentration of DMSO. For segment length measurements, water was replaced with fresh WIN-18446 after 48 h (2 dpt). Segment length was measured 2 days later (7 dpa/4 dpt). Three trials were conducted using 6–8 fish per trial.

### Statistical analysis

Statistical analysis was completed using GraphPad Prism software (9.5.1). When comparing two samples, an unpaired *t*-test was performed. When comparing three or more samples, a one-way analysis of variance (ANOVA) was performed followed by the Tukey *posthoc* analysis. Analysis of grouped knockdown (KD) replicates compared to control replicates for qPCR was performed via two-way ANOVA followed by Dunnett's multiple comparison test.

## Results

### RA acts as a genetic regulator of *cx43* and *evx1*

RA is a derivative of lipophilic Vitamin A and is synthesized locally by aldehyde dehydrogenase 1 (Aldh1) family members. In the zebrafish-regenerating fin, *aldh1a2* is expressed in the distal most blastema.<sup>16</sup> Once synthesized, RA can enter target

tissues and associate intracellularly with RA receptors (RARs) that bind to RA response elements (RAREs) and regulate gene transcription.<sup>17</sup> We first tested if *aldh1a2* is reduced at the time of joint initiation in WT fins. We monitored expression of *aldh1a2* at 72 hpa (preinitiation), 87 hpa (initiation), and 96 hpa (postinitiation) by ISH. Indeed, we found that expression of *aldh1a2* is decreased corresponding with joint-initiation (Fig. 1). While correlative, this result is consistent with the model that RA synthesis is part of the endogenous mechanism that regulates *cx43* expression during joint initiation.

To provide more direct evidence for the role of RA in influencing *cx43* and *evx1*, we next tested if inhibition of Aldh1a2 impacts *cx43* and *evx1* expression during regeneration. We utilized MO-mediated KD of Aldh1a2 to reduce protein levels. To minimize the chance of observing off-target effects, we tested two nonoverlapping MOs. We used one translation blocking MO (ATG-MO), and one splice blocking MO (SB-MO), and we compared each to the SC-MO as a negative control. To validate the MOs, we first confirmed that Aldh1a2 protein is reduced by immunoblotting (Fig. 2A, B). Next, we confirmed that reduced Aldh1a2 was sufficient to impact the expression of the known RA target *sonic hedgehog* (*shh*).<sup>18</sup> As expected, reduced Aldh1a2-KD led to ectopic expression of *shh* via ISH and aberration of the typical two-domain patterning in the regenerating fin (Fig. 2C).

We then examined *cx43* and *evx1* transcripts via ISH and qPCR (Fig. 3). Reduced Aldh1a2 also downregulated the expression of *cx43*, suggesting that RA availability promotes levels of *cx43* during regeneration. Conversely, *evx1* expression was upregulated by Aldh1a2-KD, which is consistent with the previously discovered role of RA in suppressing *evx1* expression.<sup>9</sup> These changes in gene expression were observed for both the ATG-MO and the SB-MO treated fins (SB-MO treated fins not shown), and by both ISH and qPCR. Together, these findings indicate that RA acts upstream of *cx43* and *evx1*. To test for the possibility of feedback between *aldh1a2* and *cx43*, we performed *aldh1a2* ISH and qPCR in WT and *sof*<sup>b123</sup> fins. Expression of *aldh1a2* remained unchanged in *sof*<sup>b123</sup> fins compared to WT regenerating fins using both methods (Fig. 4), indicating that RA levels are not influenced by Cx43.

### RA acts in a common pathway with Cx43 to influence joint formation

Since Aldh1a2 influences *cx43* and *evx1* expression, we next examined if Aldh1a2-KD also influences segment-

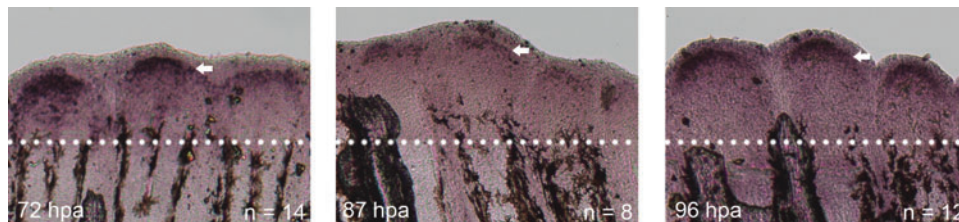


**FIG. 1.** Expression of *aldh1a2* changes during the joint-initiation timeline. Fins were amputated to the 33% level and harvested at either 72 hpa (preinitiation), 87 hpa (initiation), or 96 hpa (postinitiation). Amputation planes are denoted by the white dotted line. ISH using antisense digoxigenin-labeled probe against *aldh1a2* was used to examine relative gene expression. Expression of *aldh1a2* is localized to the distal-most blastema (white arrow). At 87 hpa *aldh1a2* expression is notably reduced, corresponding to joint initiation. Three independent trials were performed. ISH, *in situ* hybridization.

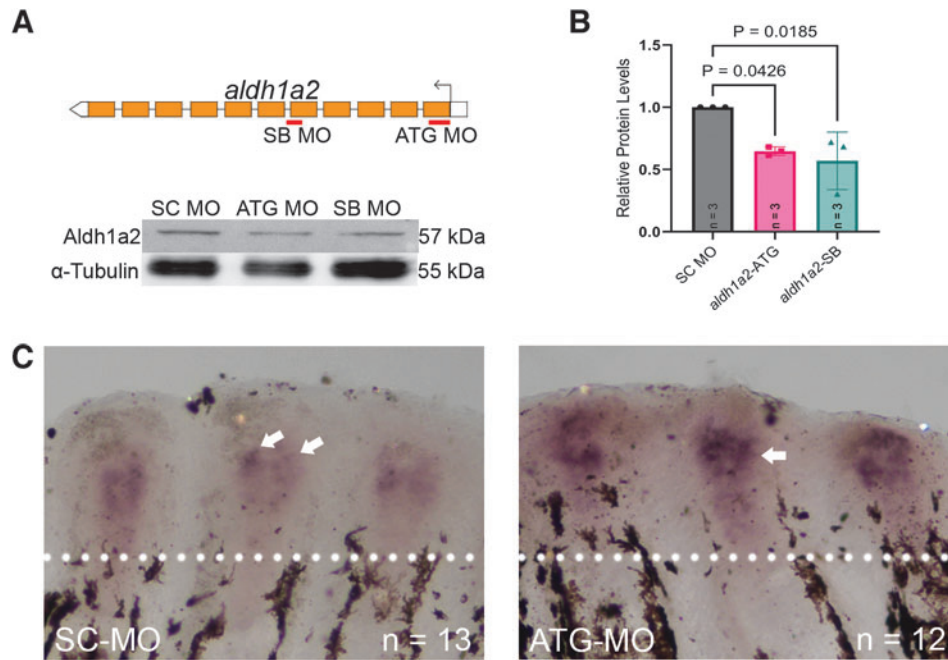


**FIG. 2.** MO-mediated KD of *Aldh1a2* reduces protein levels and disrupts *shh* expression. **(A)** Cartoon illustration of unspliced *aldh1a2* mRNA with MO binding sites denoted in red. Western blot of *Aldh1a2* protein levels shows reduced levels normalized to Tubulin loading control in both ATG-MO and SB-MO treatments. **(B)** Quantification of relative protein levels of KD fin lysates ( $n=3$  lysates of 3 pooled fins each; mean values [SC-MO=1, ATG-MO=0.65, SB-MO=0.57]). Both MO KD groups show a significant reduction in protein levels (one-way ANOVA followed by *posthoc* Tukey test). **(C)** ISH using antisense digoxigenin-labeled probe against *shh* was used to examine relative gene expression in fins injected with either SC-MO or *Aldh1a2* ATG-MO. Typical expression of *shh* is found in two distinct domains, as observed in SC-MO fins. Separation of these domains is not observed in ATG-MO fins (white arrows). Amputation planes are denoted by the white dotted line. Three independent trials were performed. ANOVA, analysis of variance; ATG-MO, one translation blocking MO; KD, knockdown; MO, morpholino; SB-MO, splice blocking MO; SC-MO, standard control MO; *shh*, *sonic hedgehog*.

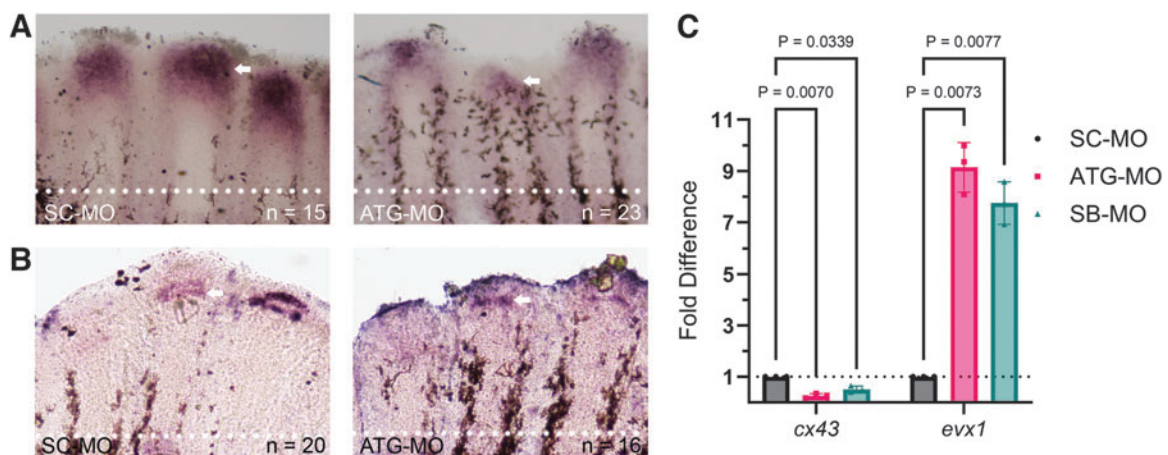


**FIG. 3.** MO-mediated KD of *Aldh1a2* decreases expression of *cx43* and increases expression of *evx1*. **(A)** ISH using antisense digoxigenin-labeled probe against *cx43* was used to examine relative gene expression in fins injected with either SC-MO or ATG-MO. Expression of *cx43* is decreased following KD of *Aldh1a2* (white arrows). **(B)** ISH using antisense digoxigenin-labeled probe against *evx1* was used to examine relative gene expression in fins injected with either SC-MO or ATG-MO. Expression of *evx1* is increased following KD of *Aldh1a2* (white arrows). Similar results were observed using the *Aldh1a2* SB-MO (not shown). Amputation planes are denoted by the white dotted line. **(C)** Gene expression levels quantified by qPCR in *aldh1a2* KD fins. Graph shows each biological replicate, mean fold difference, and standard deviation. A fold difference of one represents no change from SC-MO expression, shown by the black dotted line. Expression of *cx43* is significantly reduced in following injection of both ATG- and SB-MO, while *evx1* levels are significantly elevated in each (two-way ANOVA followed by Dunnett's multiple comparison test). Three independent trials were performed. qPCR, quantitative RT-PCR.

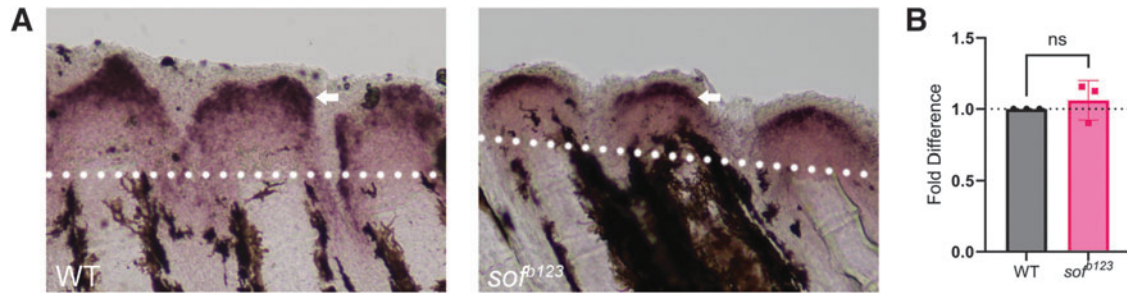


**FIG. 4.** Expression of *aldh1a2* is similar between WT and *sof<sup>b123</sup>* fins. **(A)** ISH using antisense digoxigenin-labeled probe against *aldh1a2* was used to examine relative gene expression in WT and *sof<sup>b123</sup>* regenerating fins (5 dpa). Expression levels of *aldh1a2* appear unchanged in *sof<sup>b123</sup>* compared to WT (white arrows). Amputation planes are denoted by the white dotted line. **(B)** Gene expression levels quantified by qPCR in WT versus *sof<sup>b123</sup>* fins. Graph shows each biological replicate, mean fold difference, and standard deviation. A fold difference of one represents no change from WT expression, shown by the black dotted line. Expression of *aldh1a2* in *sof<sup>b123</sup>* does not significantly differ from levels in WT (unpaired *t*-test). Three independent trials were performed. WT, wild-type.

length. To monitor changes in segment length, we inhibit gene function at 72 hpa, before joint initiation (87 hpa). Then, we evaluate segment length at 4 days posttreatment by measuring the first completed segment distal to the amputation plane. To examine the impacts of gene KD during fin regeneration, we inject/electroporate the MO (i.e., gene-targeting or control MOs) into one half of the fin, leaving the other half of the fin as an uninjected internal control.<sup>19</sup> We measure similarity of about 100% that indicates little difference between the injected and uninjected lobes.<sup>20</sup> In contrast, Aldh1a2-KD using either the ATG-MO or the SB-

MO showed a percent similarity of about 85%, compared to the near 100% similarity for the SC-MO treated fins (Fig. 5).

As an alternate means to reduce Aldh1a2 function we used the pharmacological agent WIN-18446, which inhibits enzymatic activity.<sup>21</sup> Note that because fish are treated systemically with WIN-18446/DMSO, the percent similarity method is not possible. Absolute segment length is reported instead. Following treatment beginning at 72 hpa (i.e., pre-initiation), segments were significantly shorter in the drug treated fins compared to vehicle alone (Fig. 5). Because two independent targeting MOs, as well as pharmacological

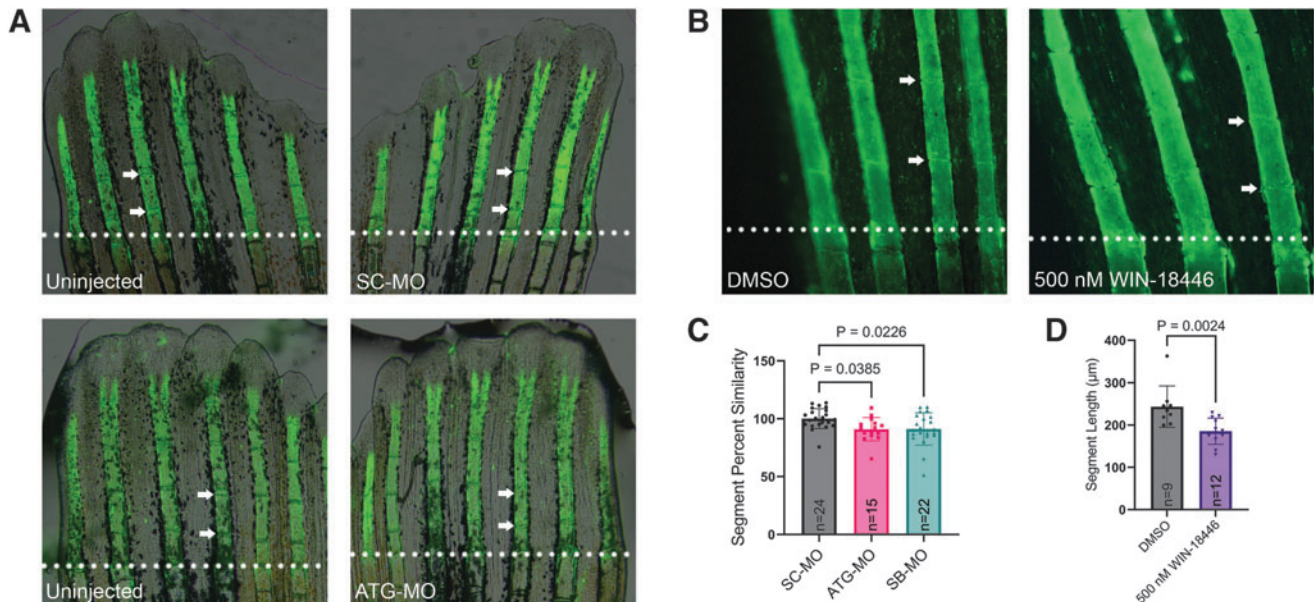


**FIG. 5.** Inhibition of Aldh1a2 reduces segment length in regenerating fins. **(A)** MO injected fins were calcein-stained and measured for segment length (white arrows). Percent similarity was calculated. Only fins for ATG-MO and SC-MO are shown. Amputation planes are denoted by the white dotted line. **(B)** Fins treated with 500 nM WIN-18446 in system water or DMSO alone were calcein-stained and measured for segment length (white arrows). All fins were amputated to the 50% level and imaged at 7 dpa/4 dpt. Amputation planes are denoted by the white dotted line. **(C)** Quantitation of the analyses of segment length in fins treated for MO-mediated KD. Both ATG-MO and SB-MO treated fins show significant reduction in segment length percent similarity compared to SC-MO (one-way ANOVA followed by *posthoc* Tukey test). **(D)** Analysis of WIN-18446 treated fins was performed by comparing segment length of treated fins compared to DMSO alone. Treatment with WIN-18446 significantly reduces segment length compared to DMSO alone (unpaired *t*-test). DMSO, dimethyl sulfoxide.

inhibition of *Aldh1a2* activity, all lead to reduced segment length, the conclusion that RA influences the timing of joint formation is well supported.

To determine if *Aldh1a2* acts in a common pathway with *cx43* to inhibit joint formation, we tested for synergy by combining subthreshold doses of WIN-18446 and *cx43* function. We found that the dose of 100 nM of WIN-18446 did not influence segment length (Fig. 6). We combined this low dose of WIN-18446 with *sof<sup>b123</sup>/+* heterozygous fish. The *sof<sup>b123</sup>/+* fins exhibit subthreshold activity of *cx43* function.<sup>5,22</sup> We observed significant reduction in segment length in the WIN-18446-treated *sof<sup>b123</sup>/+* fins compared to either 100 nM WIN-18446 (in WT-treated fish) or *sof<sup>b123</sup>/+* (plus DMSO vehicle) (Fig. 6). Taken together, these data suggest that *aldh1a2* (and therefore RA) functions in a common pathway with *cx43* to influence segment length/joint formation.

## Discussion

Prior studies revealed that *cx43* mRNA levels are transiently reduced at the time of joint initiation.<sup>8</sup> We interpret these findings to indicate that oscillations of *cx43* mRNA contribute to the functional level of Cx43-GJIC, that in turn determines the alternating pattern of bony segments and joints in the zebrafish fin. This report adds insight to this model by demonstrating that RA represents one of the endogenous mechanisms regulating *cx43* expression. First, *aldh1a2* levels are similarly reduced concomitant with joint initiation. More im-

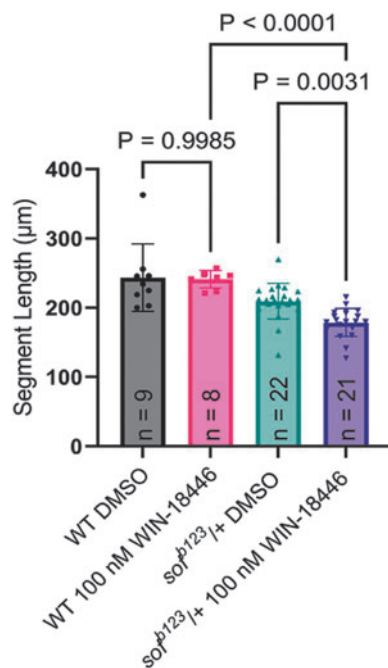


**FIG. 6.** Evidence for synergy between *aldh1a2* and *cx43*. The subthreshold dose of 100 nM WIN-18446 did not affect segment length compared to DMSO alone; *sof<sup>b123</sup>/+* heterozygous fish do not have short segments. However, *sof<sup>b123</sup>/+* regenerating fish treated with 100 nM WIN-18446 show a significant reduction in segment length compared to either *sof<sup>b123</sup>/+* with DMSO alone, or to WT fins treated with 100 nM WIN-18446 (one-way ANOVA followed by *post-hoc* Tukey test).

portantly, *Aldh1a2*-KD reduces *cx43* while increasing *evx1*. Furthermore, *Aldh1a2*-KD leads to reduced segment length and synergizes with *cx43* to influence segment length.

Before considering how RA influences segment length, we note that both RA and Cx43 are also required for cell proliferation in the regenerating fin blastema.<sup>19,23</sup> However, mechanisms regulating segment length are independent of mechanisms regulating cell proliferation (i.e., which regulates regenerate length),<sup>19,24</sup> thus precluding the possibility that the influence of RA on cell proliferation in turn alters segment length. Rather, segment length is a specific readout of the timing of joint formation.

Important questions remain regarding the role of RA on *evx1* expression and joint formation (Fig. 7). For example, Cx43-GJIC inhibits *evx1*.<sup>7,8</sup> Therefore, it is tempting to speculate that RA promotes *cx43*, and then elevated Cx43-GJIC inhibits *evx1*. However, the data presented here do not rule out the possibility that RA enters SPCs and directly inhibits *evx1* transcription. Distinguishing these possibilities will require identifying and disrupting RAREs in the regulatory regions for both *cx43* and *evx1*, and monitoring the impacts on gene expression and segment length.

Irrespective of how *evx1* expression is regulated, this article provides evidence that RA is part of the mechanism that regulates *cx43* expression levels during skeletal regeneration. This is not the only mechanism. For example, calcineurin inhibits *cx43* expression.<sup>8,25</sup> Thus, treatment with the calcineurin inhibitor FK506 leads to an upregulation of *cx43* (and loss of *evx1* and joints).<sup>8,26</sup> Interestingly, FK506 treatment also influences the expression of several RA metabolism genes, consistent with a role for calcineurin inhibiting RA signaling.<sup>25</sup> Future studies will reveal if calcineurin and RA act together or separately to regulate *cx43*.

Another way that *cx43* expression is known to be regulated is by the micro-RNA *miR133a*.<sup>8,27</sup> Interestingly, both calcineurin pathways and the *miR133a* inhibit *cx43* expression, while we find that RA promotes *cx43* expression. Therefore, these and other multiple inputs must be coordinated in time and space for *cx43* transcription to be precisely regulated during skeletal patterning. Moreover, it remains possible that

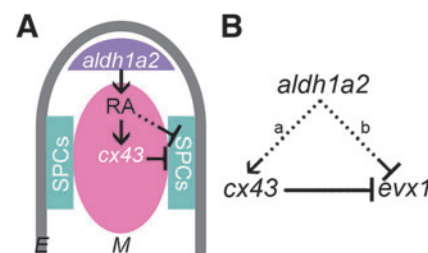


**FIG. 7.** Model for interactions between RA, *cx43*, and *evx1* in regenerating fins. (A) The gene coding for the RA-synthesizing enzyme *aldh1a2* is expressed in the cells of the distal most blastema (purple). The *cx43* gene is expressed in the cells of the proximal blastema (pink). SPCs are located lateral to the proximal blastema (cyan). RA is lipophilic and may enter cells of the proximal blastema and the lateral SPCs. E, epidermis; M, mesenchyme. (B) RA is synthesized in *aldh1a2* expressing cells, and promotes *cx43* and inhibits *evx1*. Thus, *evx1* inhibition may be the result of RA elevating *cx43* which inhibits *evx1* (a), may be due to direct inhibition (b), or both. RA, retinoic acid, SPC, skeletal precursor cell.

regulation of Cx43-GJIC also occurs at posttranscriptional levels, such as through regulation of the Cx43 half-life.<sup>28</sup> Continued studies will provide critical insights into the collection of Cx43 regulatory pathways, and their regulation, in the fin skeleton.

### Conclusions

We suggest that oscillations of Cx43-GJIC are responsible for the alternating pattern of bony segments and joints in the regenerating zebrafish fin. Prior research identified reduction of *cx43* mRNA levels coincident with joint initiation. Therefore, mechanisms regulating *cx43* transcription likely contribute to the periodic abrogation of Cx43-GJIC. Here, we demonstrate that RA promotes *cx43* expression and is required for the appropriate length of fin ray segments. Future studies will focus on understanding how RA signaling is coordinated with other pathways that regulate *cx43* mRNA levels and on how RA regulates the expression of *evx1*.

### Acknowledgments

The authors wish to thank Rebecca Bowman and Nicole Barbera for care of the zebrafish colony. We also thank members of the Iovine lab for their thoughtful contributions to this research.

### Authors' Contributions

A.W.S. performed experiments, completed data analysis, prepared figures, and contributed to writing (review and editing). N.S.W. performed experiments, completed data analysis, and contributed to writing (editing). M.K.I. contributed to manuscript writing (review and editing) and supervision. All coauthors have reviewed and approved this article.

### Author Disclosure Statement

No competing financial interests exist.

### Funding Information

This work was supported by NIH-2R15-HD080507 (M.K.I.), by the Lehigh University Nemes Fellowship (A.W.S.), and by the Lehigh Grant for Experiential Learning in Health (N.S.W.).

### References

- Wehner D, Weidinger G. Signaling networks organizing regenerative growth of the zebrafish fin. *Trends Genet* 2015;31(6):336–343; doi: 10.1016/j.tig.2015.03.012
- Tu S, Johnson SL. Fate restriction in the growing and regenerating zebrafish fin. *Dev Cell* 2011;20(5):725–732; doi: 10.1016/j.devcel.2011.04.013
- Ton QV, Iovine MK. Identification of an *evx1*-dependent joint-formation pathway during FIN regeneration. *PLoS One* 2013;8(11):e81240; doi: 10.1371/journal.pone.0081240
- Schulte CJ, Allen C, England SJ, et al. *Evx1* is required for joint formation in zebrafish fin dermoskeleton. *Dev Dyn* 2011;240(5):1240–1248; doi: 10.1002/dvdy.22534
- Iovine MK, Higgins EP, Hindes A, et al. Mutations in connexin43 (GJA1) perturb bone growth in zebrafish fins. *Dev Biol* 2005;278(1):208–219; doi: 10.1016/j.ydbio.2004.11.005
- Warner A, Clements DK, Parikh S, et al. Specific motifs in the external loops of connexin proteins can determine gap junction formation between chick heart myocytes. *J Physiol* 1995;488 (Pt 3):721–728; doi: 10.1113/jphysiol.1995.sp021003
- Bhattacharya S, Hyland C, Falk MM, et al. Connexin 43 gap junctional intercellular communication inhibits *evx1* expression and joint formation in regenerating fins. *Development* 2020;147(13):dev190512; doi: 10.1242/dev.190512
- Dardis G, Tryon R, Ton Q, et al. Cx43 suppresses *evx1* expression to regulate joint initiation in the regenerating fin. *Dev Dyn* 2017;246(9):691–699; doi: 10.1002/dvdy.24531
- McMillan SC, Zhang J, Phan HE, et al. A regulatory pathway involving retinoic acid and calcineurin demarcates and maintains joint cells and osteoblasts in regenerating fin. *Development* 2018;145(11):dev161158; doi: 10.1242/dev.161158
- Lee Y, Hami D, De Val S, et al. Maintenance of blastemal proliferation by functionally diverse epidermis in regenerating zebrafish fins. *Dev Biol* 2009;331(2):270–280; doi: 10.1016/j.ydbio.2009.05.545
- Ton QV, Iovine MK. Semaphorin3d mediates Cx43-dependent phenotypes during fin regeneration. *Dev Biol* 2012;366(2):195–203; doi: 10.1016/j.ydbio.2012.03.020
- Sanchez AC, Thren ED, Iovine MK, et al. *Esco2* and cohesin regulate CRL4 ubiquitin ligase *ddb1* expression and thalidomide teratogenicity. *Cell Cycle* 2022;21(5):501–513; doi: 10.1080/15384101.2021.2023304
- Thummel R, Kathryn Iovine M. Using morpholinos to examine gene function during fin regeneration. *Methods Mol Biol* 2017;1565:79–85; doi: 10.1007/978-1-4939-6817-6\_7
- Du SJ, Frenkel V, Kindschi G, et al. Visualizing normal and defective bone development in zebrafish embryos using the fluorescent chromophore calcein. *Dev Biol* 2001;238(2):239–246; doi:10.1006/dbio.2001.0390
- Iovine MK, Johnson SL. Genetic analysis of isometric growth control mechanisms in the zebrafish caudal Fin. *Genetics* 2000;155(3):1321–1329.
- Blum N, Begemann G. Osteoblast de- and redifferentiation are controlled by a dynamic response to retinoic acid during zebrafish fin regeneration. *Development* 2015;142(17):2894–2903; doi: 10.1242/dev.120204
- Rhinn M, Dolle P. Retinoic acid signalling during development. *Development* 2012;139(5):843–858; doi: 10.1242/dev.065938
- Laforest L, Brown CW, Poleo G, et al. Involvement of the sonic hedgehog, patched 1 and *bmp2* genes in patterning of the zebrafish dermal fin rays. *Development* 1998;125(21):4175–4184; doi: 10.1242/dev.125.21.4175
- Hoptak-Solga AD, Nielsen S, Jain I, et al. Connexin43 (GJA1) is required in the population of dividing cells during fin regeneration. *Dev Biol* 2008;317(2):541–548; doi: 10.1016/j.ydbio.2008.02.051
- Bhadra J, Iovine MK. *Hsp47* mediates Cx43-dependent skeletal growth and patterning in the regenerating fin. *Mech Dev* 2015;138 Pt 3:364–374; doi: 10.1016/j.mod.2015.06.004
- Paik J, Haenisch M, Muller CH, et al. Inhibition of retinoic acid biosynthesis by the bisdichloroacetyldiamine WIN 18,446 markedly suppresses spermatogenesis and alters retinoid metabolism in mice. *J Biol Chem* 2014;289(21):15104–15117; doi: 10.1074/jbc.M113.540211

22. Banerji R, Skibbens RV, Iovine MK. Cohesin mediates Esco2-dependent transcriptional regulation in a zebrafish regenerating fin model of Roberts Syndrome. *Biol Open* 2017;6(12):1802–1813; doi: 10.1242/bio.026013
23. Blum N, Begemann G. Retinoic acid signaling controls the formation, proliferation and survival of the blastema during adult zebrafish fin regeneration. *Development* 2012;139(1):107–116; doi: 10.1242/dev.065391
24. Sims K Jr., Eble DM, Iovine MK. Connexin43 regulates joint location in zebrafish fins. *Dev Biol* 2009;327(2):410–418; doi: 10.1016/j.ydbio.2008.12.027
25. Kujawski S, Lin W, Kitte F, et al. Calcineurin regulates coordinated outgrowth of zebrafish regenerating fins. *Dev Cell* 2014;28(5):573–587; doi: 10.1016/j.devcel.2014.01.019
26. Daane JM, Lanni J, Rothenberg I, et al. Bioelectric-calcineurin signaling module regulates allometric growth and size of the zebrafish fin. *Sci Rep* 2018;8(1):10391; doi: 10.1038/s41598-018-28450-6
27. Yin VP, Lepilina A, Smith A, et al. Regulation of zebrafish heart regeneration by miR-133. *Dev Biol* 2012;365(2):319–327; doi: 10.1016/j.ydbio.2012.02.018
28. Thevenin AF, Kowal TJ, Fong JT, et al. Proteins and mechanisms regulating gap-junction assembly, internalization, and degradation. *Physiology (Bethesda)* 2013;28(2):93–116; doi: 10.1152/physiol.00038.2012

Address correspondence to:

*M. Kathryn Iovine, PhD*  
*Department of Biological Sciences*  
*Lehigh University*  
*111 Research Drive, Iacocca D222*  
*Bethlehem, PA 18015*  
*USA*

*Email: mki3@lehigh.edu*